High-Latitude Topside Ionospheric Vertical Electron-Density-Profile changes in response to Large Magnetic Storms

Robert F. Benson[1], Joseph Fainberg[1], Vladimir A. Osherovich[2], Vladimir Truhlik[3], Yongli Wang[4], Dieter Bilitza[5], and Shing F. Fung[1]

[1]NASA/Goddard Space Flight Center, Geospace Physics Laboratory, Code 673, Heliophysics Science Division, Greenbelt, MD 20771
[2]CUA/Goddard Space Flight Center, Geospace Physics Laboratory, Code 673, Heliophysics Science Division, Greenbelt, MD 20771
[3]Institute of Atmospheric Physics, Academy of Sciences of the Czech Republic, Praha, Czech Republic
[4]UMBC/GPHI/Space Weather Laboratory, Code 674, Heliophysics Science Division, Greenbelt, MD 20771
[5]GMU/SWL/Heliospheric Physics Laboratory, Code672 Heliophysics Science Division, Greenbelt, MD 20771

ABSTRACT

Large magnetic-storm induced changes have been detected in high-latitude topside vertical electron-density profiles $N_e(h)$. The investigation was based on the large database of topside $N_e(h)$ profiles and digital topside ionograms from the International Satellites for Ionospheric Studies (ISIS) program available from the NASA Space Physics Data Facility (SPDF) at http://spdf.gsfc.nasa.gov/isis/isis-status.html. This large database enabled $N_e(h)$ profiles to be obtained when an ISIS satellite passed through nearly the same region of space before, during, and after a major magnetic storm. A major goal was to relate the magnetic-storm induced high-latitude $N_e(h)$ profile changes to solar-wind parameters. Thus an additional data constraint was to consider only storms where solar-wind data were available from the NASA/SPDF OMNIWeb database. Ten large magnetic storms (with Dst less than -100 nT) were identified that satisfied both the $N_e(h)$ profile and the solar-wind data constraints. During five of these storms topside ionospheric $N_e(h)$ profiles were available in the high-latitude northern-hemisphere and during the other five storms similar ionospheric data were available in the southern hemisphere. Large $N_e(h)$ changes were observed during each one of these storms. Our concentration in this paper is on the northern hemisphere. The data coverage was best for the northern-hemisphere winter. Here $N_e(h)$ profile enhancements were always observed when the magnetic local time (MLT) was within 3 hours of midnight and $N_e(h)$ profile depletions were always observed when the MLT was within 3 hours of noon. The observed $N_e(h)$ deviations were compared with solar-wind parameters, with appropriate time shifts, for four storms.

1. INTRODUCTION

While there have been investigations over many decades of the responses of the topside ionosphere to magnetic storms, e.g., see the review by *Warren* [1969] in the June,

1969 Proc. IEEE special issue dedicated to the International Satellites for Ionospheric Studies (ISIS) program, we seek to determine if such responses can be directly related to solar-wind parameters. More recent works have also addressed this goal, e.g., [*Chen et al.*, 2014; *Field and Rishbeth*, 1997; *Fuller-Rowell et al.*, 1994; *Horvath and Lovell*, 2014; *Kitamura et al.*, 2010; *Liu et al.*, 2010; *Murr and Hughes*, 2007; *Prölss*, 2011; *Rodger et al.*, 1989; *Ruohoniemi et al.*, 2002; *Sojka and Schunk*, 1983; *Yizengaw et al.*, 2006].

The motivation for this work was provided by magnetospheric electron-density (N_e) determinations during a large magnetic storm using data from the Radio Plasma Imager (RPI) on the IMAGE satellite. The RPI detected large magnetic-storm-enhanced N_e values, which were highly correlated with fluctuations in solar-wind parameters, when IMAGE was ~ $8R_E$ above the northern polar cap [*Osherovich et al.*, 2007]. Profile inversions of RPI magnetic field-aligned echoes indicated that these N_e enhancements extended down to about 4 R_E in radial distance [*Tu et al.*, 2007]. Our goal here is to extend such high-latitude investigations to even lower altitudes, i.e., into the topside ionosphere, in an attempt to relate changes in vertical electron-density profiles $N_e(h)$ to solar-wind parameters during large magnetic storms. Ten large magnetic storms (Dst < -100 nT) were identified where high-latitude topside vertical electron-density profiles $N_e(h)$ could be obtained from Alouette/ISIS topside-sounder data and where solar-wind data were available. Large $N_e(h)$ changes were observed during the storms in all cases. Topside-ionospheric $N_e(h)$ profiles were available in the high-latitude northern hemisphere during five of these storms and in the southern hemisphere during the other five storms. The Alouette/ISIS topside-sounder data and the solar-wind data were obtained from the NASA Space Physics Data Facility (SPDF); the solar-wind data from their OMNI database. Here we concentrate on the changes observed during four of the northern hemisphere storms where, in addition to good $N_e(h)$ profiles before, during, and after the storms, there was good coverage of solar-wind data with what we considered to be the appropriate time shift.

2. High-latitude topside $N_e(h)$ profile changes during large magnetic storms

In order to detect magnetic-storm-induced $N_e(h)$ changes it is necessary to have observations within the same small region of space before, during, and after a major magnetic storm. Such an investigation requires a large database. Here we selected restricted regions of magnetic local time (MLT), magnetic latitude (MLAT) and geographic longitude (GLON) for each storm investigated. The restrictions on the parameter ranges were critical since too broad a range reduces the significance of the results and too small a range leads to insufficient coverage. The $N_e(h)$ profiles for the first storm investigated were based on the hand-scaling of 35-mm film ionograms by skilled observers in the 1960s and 1970s during the peak activity of the ISIS program. They were obtained from the SPDF at ftp://spdf.gsfc.nasa.gov/pub/data. This was a large magnetic storm, as indicated by the Dst profile in the left panel of Figure 1, and it produced profound nighttime and daytime topside $N_e(h)$ changes as illustrated in the center and right panels, respectively.
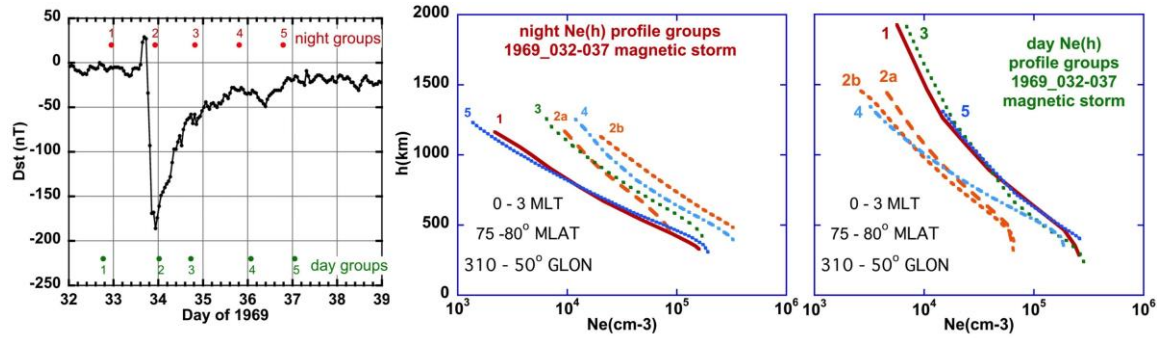
Figure 1. (left) Dst profile from the large magnetic storm during the 1969 interval from days 32 – 39 with the times for 5 groups of N_e(h) profiles indicated at the top for night conditions (center panel) and at the bottom for day conditions (right panel). The profiles in the center and right panels are labeled according to the times they were collected (indicated on left panel) as they passed through the restricted region indicated in the lower left of each panel. Each profile corresponds to a single representative profile of a group of profiles collected at the time during the storm indicated in the left panel. If there were significant differences within a group two representative profiles are presented (as is the case for group 2 during the Dst minimum).

The main features to notice in Figure 1 are the following:
(1) profiles 1 and 5 nearly coincide (before & after the storm, respectively)
(2) profile 2 (during Dst minimum) shows increase (decrease) during night (day)
(3) bifurcation of the group-2 profiles implies strong Ne gradients during Dst minimum
(4) profiles 3 and 4 are more consistently displaced during night than day.
The time separations between profiles 2a and 2b are 84 s and 39 s in the center (night) and right (day) panels, respectively, indicating rapid change in the topside ionosphere during the time of minimum Dst.

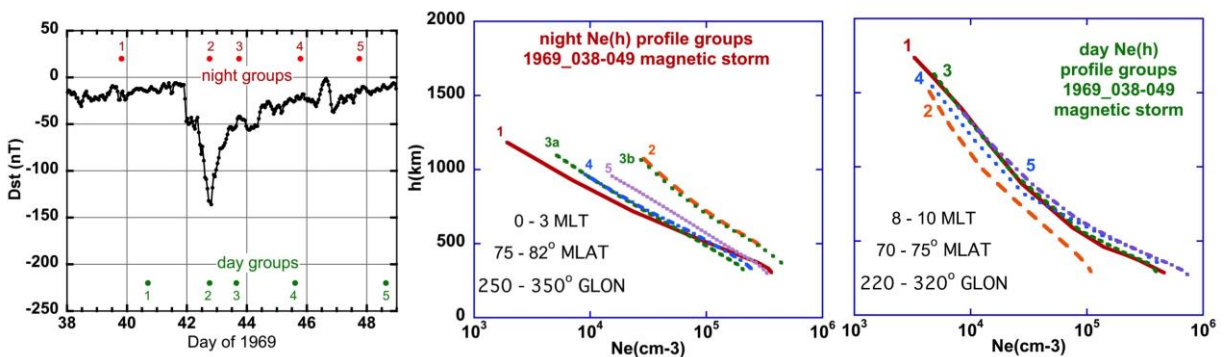A similar presentation for the second storm investigated is presented in Figure 2.

Figure 2. Same as Figure 1 except for the magnetic storm during the 1969 interval from days 38 – 49.

Again, there is a large increase in the N_e(h) profiles near the Dst minimum compared with pre-storm conditions (profile #2 compared with profile #1) at night (center panel) and a decrease during the day (right panel). Also, rapid changes are again indicated at night. In this case however, the greatest changes are observed early in the recovery stage

where the large changes in the group-3 profiles, in the center panel of Figure 2, occur during the 30 s time separation between profiles 3a and 3b. (Profile #3b essentially coincides with profile #2.) These changes are likely due to a mixture of temporal and spatial effects since the topside sounder travels about 200 km in that time interval. The disturbed nature of this nighttime region is also indicated by the failure of the profiles, even as late as profile #5, to return to the pre-storm conditions of profile #1. In contrast, the daytime profiles (right panel) return to nearly pre-storm conditions after profile #2.

Two additional large magnetic storms, both corresponding to northern-hemisphere spring daytime conditions were investigated in detail. The Dst plots for these storms, and the locations where topside ionospheric $N_e(h)$ profiles were obtained, are presented in Figure 3. In this case the profiles were determined from the manual scaling of digital topside ionograms from ISIS 1 and ISIS 2. These ionograms were obtained from http://spdf.gsfc.nasa.gov/isis/isis-status.html; they are also available from the Virtual Wave Observatory [*Fung*, 2010].
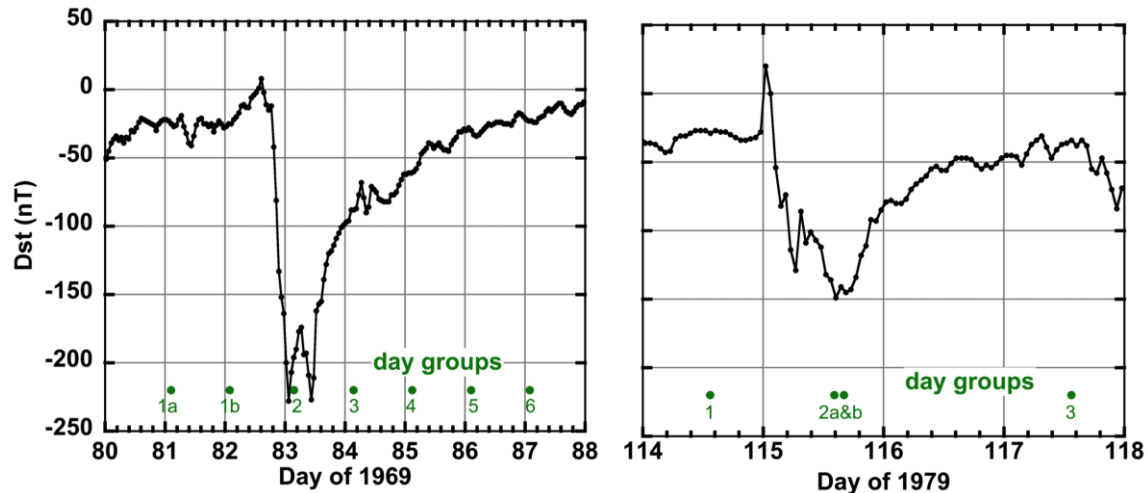

Figure 3. Dst and the locations of $N_e(h)$ profiles derived from digital topside ionograms from ISIS 1, for the 1969 storm corresponding to the left panel, and ISIS 2 for the 1979 storm corresponding to the right panel.

The northern-hemisphere daytime $N_e(h)$ profiles for the storms indicated in Figure 3 show large decreases near the Dst minima as were observed for the northern-hemisphere winter storms of Figures 1 and 2. The decreases were observed for groups 2 and 3 during the 1969 storm (Figure 3, left panel) and for groups 2a and 2b during the 1979 storm (Figure 3, right panel); they were observed to be even larger in these spring storms, than during the winter storms of Figures 1 and 2, as will be illustrated in Section 3.

3. Relating magnetic-storm-induced $N_e(h)$ profile changes to solar-wind velocity

Figure 4 presents the solar wind data from OMNI 2 [*King and Papitashvili*, 2004] during the large magnetic storm indicated by the left panel of Figure 1. The behavior of the absolute value B of the total solar-wind magnetic field **B** (top panel), the components

of **B** in the middle panel, and the absolute value v of the solar-wind velocity **v** (lower panel) have the characteristics of solar-wind magnetic clouds [*Burlaga et al.*, 1981; *Osherovich and Burlaga*, 1997]. Note that in this case v, which is considered to be the most effective geo-effective parameter, see, e.g., [*Osherovich and Fainberg*, 2015], reaches a maximum near 700 km/s. In order to relate v to the observed large changes in the $N_e(h)$ profiles, presented in Section 2, it is necessary to obtain some way of estimating the appropriate time shift to be applied to the solar-wind data.
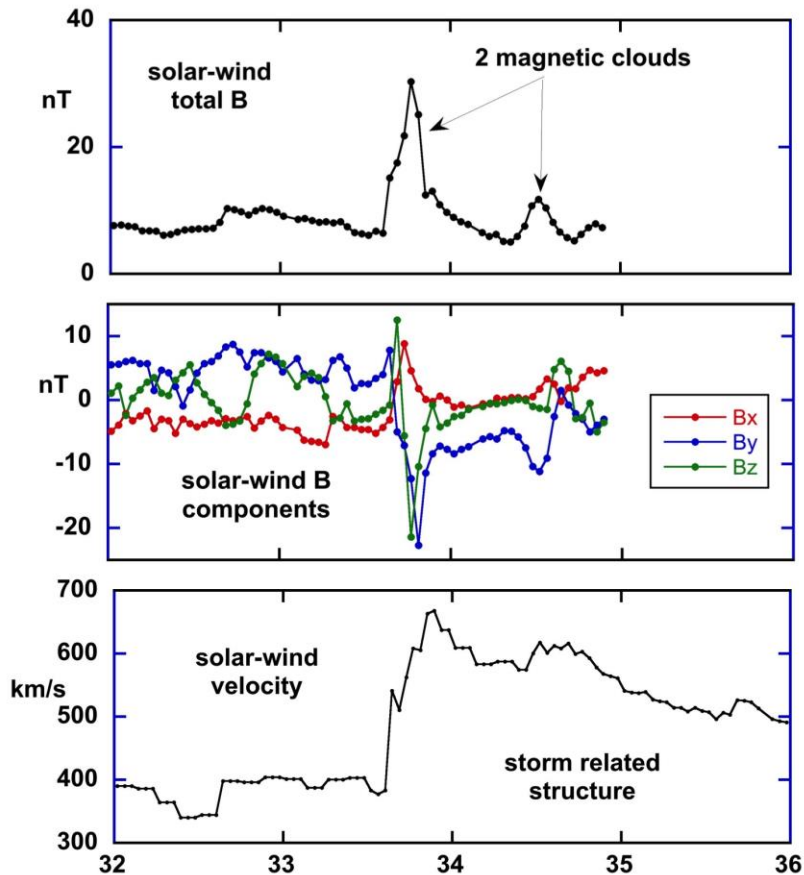

Figure 4. Solar-wind data providing evidence of magnetic clouds responsible for the magnetic storm indicated by the left panel of Figure 1.

In the work of *Osherovich et al.* [2007] there were several hours of magnetospheric N_e data near the IMAGE apogee available to compare with a similar time interval of solar-wind data. This long time span enabled the time shift between the solar wind and magnetospheric N_e observations to be determined that yielded the best correlation between the two datasets. The time shift was determined to be about 3 hr. The present investigation, involving topside ionospheric satellite observations, does not contain such long time intervals of data from a particular restricted region. Thus a different approach was used in order to provide a reasonable estimate of the proper time shift to use between solar-wind structures and the possibly related topside-ionospheric changes. This approach is described in a companion paper [*Osherovich and Fainberg*, 2015] where it was found that a time shift of 3.6 hr, or 0.15 days, would be a suggested value for the storms

investigated here. Their analysis was based on all 10 large magnetic storms identified in the present project where both the appropriate topside-sounder data and solar wind data were available.

As an indication of the degree of N_e change during the storms of Figures 1, 2, and 3 a common altitude near the upper limit of the profiles in the winter storms of Figures 1 and 2, and the spring storms of Figure 3, was selected; this altitude was 1,000 km in the former and 700 km in the latter. The ratio of N_e for group 2 to group 1 at the chosen altitude was calculated and compared to v (shifted by 0.15 day); the results are presented in Figure 5. The ratio is very large for the two winter nighttime conditions (left panel). It is less than one for the two winter daytime conditions (left panel) and for the two spring daytime conditions (right panel). These limited data samples do not suggest a direct relationship to v.
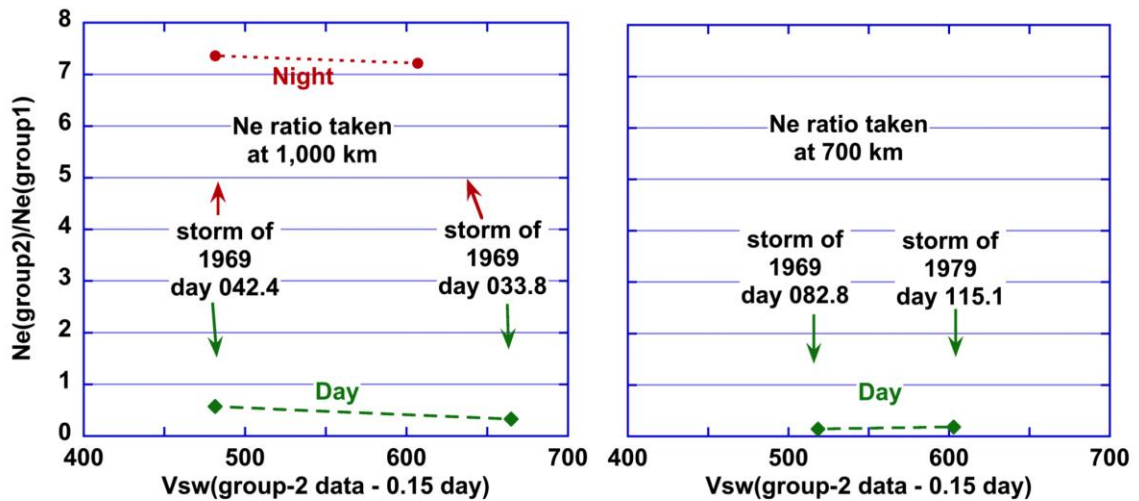

Figure 5. The ratio of N_e(group 2)/N_e(group 1) at the indicated altitudes for the magnetic storms of Figures 1, 2, and 3 vs. the absolute magnitude of the solar-wind velocity v. The storm times given correspond to the times when Dst first crosses -50 nT. The daytime ratios are, from left to right, 0.57, 0.33, 0.14, and 0.18.

4. Summary

Large high-latitude ionospheric topside N_e(h) changes were observed in the northern hemisphere during 4 large storms (Dst < -100 nT) investigated in detail. The magnetic-storm-induced changes in the winter N_e(h) profiles produced large N_e enhancements during the night and depletions during the day in two of the storms. The other two storms corresponded to spring conditions and only daytime topside profiles were available; strong magnetic-storm-induced depletions were observed in these cases. Nighttime enhancements at 1,000 km exceeded a factor of 7 and daytime depletions at 700 km approached 0.1. Rapid changes (on the order of a minute or less) were observed in the N_e(h) profiles recorded near the time of Dst minimum and, in one case, during the early recovery phase. No apparent relation between these enhancements and depletions with the absolute magnitude of the time-shifted solar-wind velocity was found in this limited data set and more work is required to see if magnetic-storm-induced high-latitude

ionospheric topside $N_e(h)$ changes can be directly related to solar-wind parameters.

References
Burlaga, L. F., E. Sittler, F. Mariani, and R. Schwenn (1981), Magnetic loop behind an interplanetary shock: Voyager, Helios, and IMP 8 observations, *J. Geophys. Res.*, *86*, 6673-6684.

Chen, G. M., J. Xu, W. Wang, J. Lei, and S.-R. Zhang (2014), The responses of ionospheric topside diffusive fluxes to two geomagnetic storms in October 2002, *J. Geophys. Res.*, *119*, doi:10.1002/2014JA020013.

Field, P. R., and H. Rishbeth (1997), The response of the ionospheric F2-layer to geomagnetic activity: an analysis of worldwide data, *J. Atmos. Solar-Terr. Phys.*, *59*, 163-180.

Fuller-Rowell, T. J., M. V. Codrescu, R. J. Moffett, and S. Quegan (1994), Response of the thermosphere and ionosphere to geomagnetic storms, *J. Geophys. Res.*, *99*, 3893-3914.

Fung, S. F. (2010), The Virtual Wave Observatory (VWO): A portal to heliophysics wave data, *Radio Sci. Bulletin*, *No. 332*, 89-102.

Horvath, I., and B. Lovell (2014), Large plasma density enhancements occurring in the northern polar region during the 6 April 2000 superstorm, *J. Geophys. Res.*, *119*, doi:10.1002/2014JA019917.

King, J. H., and N. E. Papitashvili (2004), Solar wind spatial scales and comparisons of hourly Wind and ACE plasma and magnetic field data, *J. Geophys. Res.*, *110*(A2), A02209, doi:02210.01029/02004JA010804.

Kitamura, N., Y. Nishimura, T. Ono, A. Kumamoto, A. Shinbori, M. Iizima, A. Matsuoka, and M. R. Hairston (2010), Temporal variations and spatial extent of the electron density enhancements in the polar magnetosphere during geomagnetic storms, *J. Geophys. Res.*, *115*, A00J02, doi:10.1029/2009JA014499.

Liu, J., L. Liu, B. Zhao, W. Wan, and R. A. Heelis (2010), Response of the topside ionosphere to recurrent geomagnetic activity, *J. Geophys. Res.*, *115*, A12327, doi:12310.11029/12010JA015810.

Murr, D. L., and W. J. Hughes (2007), The coherence between the IMF and high-latitude ionospheric flows: The dayside magnetosphere-ionosphere low-pass filter, *J. Atmos. Solar-Terr. Phys.*, *69*, 223-233.

Osherovich, V. A., and L. F. Burlaga (1997), Magnetic Clouds, in *Coronal Mass Ejections, Geophysical Monograph 99*, edited by N. Crooker, J. A. Joselyn and J. Feynman, pp. 157-168, American Geophysical Union, Washington.

Osherovich, V. A., and J. Fainberg (2015), Time delay between Dst index and magnetic storm related structure in the solar wind, *IES2015*.

Osherovich, V. A., R. F. Benson, J. Fainberg, J. L. Green, L. Garcia, S. Boardsen, N. Tsyganenko, and B. W. Reinisch (2007), Enhanced high-altitude polar-cap plasma and magnetic-field values in response to the interplanetary magnetic cloud that caused the great storm of 31 March 2001: A case study for a new magnetospheric index, *J. Geophys. Res.*, *112*, A06247, doi:06210.01029/02006JA012105.

Prölss, G. (2011), Density perturbations in the upper atmosphere caused by the dissipation of solar wind energy, *Surv. Geophys.*, *32*, 101-195.

Rodger, A. S., G. L. Wrenn, and H. Rishbeth (1989), Geomagnetic storms in the Antarctic F-reion. II. Physical interpretation, *J. Atmos. Terr. Phys.*, *51*, 851-866.

Ruohoniemi, J. M., S. G. Shepherd, and R. A. Greenwald (2002), The response of the high-latitude ionosphere to IMF variations, *J. Atmos. Solar-Terr. Phys.*, *64*, 159-171.

Sojka, J. J., and R. W. Schunk (1983), A theoretical study of the high-latitude F-region's response to magnetospheric storm inputs, *J. Geophys. Res.*, *88*, 2112-2122.

Tu, J.-N., M. Dhar, P. Song, B. W. Reinisch, J. L. Green, R. F. Benson, and A. J. Coster (2007), Extreme polar cap density enhancements along magnetic field lines during an intense geomagnetic storm, *J.Geophys. Res*, *112*, A05201, doi:05210.01029/02006JA012034.

Warren, E. S. (1969), The topside ionosphere during geomagnetic storms, *Proc. IEEE*, *57*(6), 1029-1036.

Yizengaw, E., M. B. Moldwin, A.Komjathy, and A. J. Mannucci (2006), Unusual topside ionospheric density response to the November 2003 superstorm, *J. Geophys. Res.*, *111*, A02308, doi:02310.01029/02005JA011433.